



Molecular Crystals and Liquid Crystals

Publication details, including instructions for authors and subscription information:

<http://www.tandfonline.com/loi/gmcl20>

Preparation and Characterization of $\text{Nd}_2\text{Fe}_{14}\text{B}/\alpha\text{-Fe}$ Nanocomposite Magnetic Material by Reduction Diffusion Process

Hyun Gil Cha^a, Young Hwan Kim^a, Chang Woo Kim^a, Young Soo Kang^a & Hae Woong Kwon^b

^a Department of Chemistry, Pukyong National University, Nam-gu, Busan, Korea

^b School of Materials Science and Engineering, Pukyong National University, Busan, Korea

Version of record first published: 22 Sep 2010

To cite this article: Hyun Gil Cha, Young Hwan Kim, Chang Woo Kim, Young Soo Kang & Hae Woong Kwon (2007): Preparation and Characterization of $\text{Nd}_2\text{Fe}_{14}\text{B}/\alpha\text{-Fe}$ Nanocomposite Magnetic Material by Reduction Diffusion Process, *Molecular Crystals and Liquid Crystals*, 464:1, 127/[709]-135/[717]

To link to this article: <http://dx.doi.org/10.1080/15421400601030563>

PLEASE SCROLL DOWN FOR ARTICLE

Full terms and conditions of use: <http://www.tandfonline.com/page/terms-and-conditions>

This article may be used for research, teaching, and private study purposes. Any substantial or systematic reproduction, redistribution, reselling, loan,

sub-licensing, systematic supply, or distribution in any form to anyone is expressly forbidden.

The publisher does not give any warranty express or implied or make any representation that the contents will be complete or accurate or up to date. The accuracy of any instructions, formulae, and drug doses should be independently verified with primary sources. The publisher shall not be liable for any loss, actions, claims, proceedings, demand, or costs or damages whatsoever or howsoever caused arising directly or indirectly in connection with or arising out of the use of this material.

Preparation and Characterization of $\text{Nd}_2\text{Fe}_{14}\text{B}/\alpha\text{-Fe}$ Nanocomposite Magnetic Material by Reduction Diffusion Process

Hyun Gil Cha
Young Hwan Kim
Chang Woo Kim
Young Soo Kang

Department of Chemistry, Pukyong National University, Nam-gu, Busan, Korea

Hae Woong Kwon

School of Materials Science and Engineering, Pukyong National University, Busan, Korea

Thermal decomposition process was applied to synthesize Fe_3O_4 and $\text{Nd}_2\text{Fe}_{14}\text{B}$ nanoparticles which were prepared by reduction diffusion process for preparing exchange-coupled nanoparticles. The magnetic $\text{Nd}_2\text{Fe}_{14}\text{B}$ nanoparticles used in this study as the starting materials were synthesized via metal oleate complex method. Also mechanical ball mill technique was applied to the mixture of magnetic $\text{Nd}_2\text{Fe}_{14}\text{B}$ and $\alpha\text{-Fe}$ nanoparticles to build an exchange-coupled nanoparticle. The mixture of $\text{Nd}_2\text{Fe}_{14}\text{B}/\alpha\text{-Fe}$ of nanoparticle was confirmed by transmission electron microscopy (TEM). The crystal structure of nanoparticle was characterized by X-ray diffraction pattern (XRD). The magnetic properties were characterized with saturation magnetization from hysteresis loop by vibrating sample magnetometer (VSM). Thermogravimetry using a microbalance with magnetic field gradient positioned below the sample was used for the measurement of a thermomagnetic analysis (TMA) curve showing the downward magnetic force versus temperature.

Keywords: exchange-coupled nanoparticles; Metal-oleate complex; $\text{Nd}_2\text{Fe}_{14}\text{B}/\alpha\text{-Fe}$ nanocomposite

This work was supported by Korean National Research Laboratory Program. H. G. Cha would like to thank the financial support by Brain Korea 21.

Address correspondence to Young Soo Kang, Department of Chemistry, Pukyong National University, 599-1 Daeyeon-3-dong, Nam-gu, Busan 608-739, Korea. E-mail: yskang@pknu.ac.kr

INTRODUCTION

Permanent magnets play an important role in today's technology. The first magnets, made from carbon steel, had energy product of only about 1 kJm^{-3} . The modern history of permanent magnets started in 1940 with the introduction of Alnico. With the introduction of Alnico, it became possible to replace electromagnets with permanent magnets, and the use of magnets started to replace electromagnets with permanent magnets, and the use of magnets started to become widespread in devices such as motors, generators or loudspeakers. The number of magnetic devices is growing each year. Stronger and smaller permanent magnets allow the construction of smaller devices that consume less energy [1–3].

Recently, considerable attention has been focused on the magnetic properties of nanostructured Fe-rich rare-earth magnet alloy. These materials show promise as permanent magnets because they exhibit a remanent magnetic polarization greater than the Stoner-Wohlfarth value of $J_s/2$ (where J_s is the saturation magnetic polarization) and offer the advantage of low cost, due to the low rare-earth content. In the absence of intercrystalline exchange coupling, the remanent magnetic polarization J_r of an isotropic magnetic material consisting of a random array of magnetic particles, exhibiting uniaxial magnetocrystalline anisotropy, should equal one half of the saturation magnetic polarization J_s , i.e. the reduced remanent magnetic polarization $\alpha = J_r/J_s = 0.5$ (Stoner-Wohlfarth theory). Recent studies have reported significantly higher values of J_r , and hence values of a greater than 0.5, in nanocomposite two-phase mixtures consisting of magnetically hard and soft phases [1].

Remanence enhancement has been reported in a variety of nanostructured Fe-rich rare earth magnet alloys, prepared by the recrystallization either of melt-spun [4–6] or of mechanically alloyed materials [7–10]. The development of high remanent magnetic polarization and a technologically useful intrinsic coercivity requires the formation of an optimum microstructure consisting of a nanocomposite two-phase mixture of magnetically hard and soft phases. The ultrafine soft magnetic grains, of high saturation magnetic polarization, enhance the low remanent magnetic polarization of the hard phase by a form of exchange coupling. Micromagnetic calculations by Schrefl *et al.*, on cellular structures in two and three dimensions have shown that the size of the soft grains should ideally be about twice of domain wall width (δ_w) of the hard magnetic phase ($\sim 8 \text{ nm}$). Skomski obtained a maximum energy product $(BH)_{\text{max}}$ of up to $1 \text{ MJ} \cdot \text{m}^{-3}$ for a multi-layer composed of alternating layers of oriented hard $\text{Sm}_2\text{Fe}_{17}\text{N}_3$

skeleton phase and a soft Fe₆₅Co₃₅ phase, but so far there has been no practical realization of such a structure. Minimization of the exchange energy tends magnetic moments in the material to align parallel to each other whereas the anisotropy energy becomes minimum, when the magnetic are parallel to the crystallographic easy magnetization direction in each grain. When grains are small enough the exchange length from crystallites oriented favorably with their easy magnetization axes to the external magnetic field covers substantial parts of neighboring grains. This leads to some proportion of magnetic anisotropy in the material and to the enhanced remanent magnetic polarization.

In this study, monodispersed iron oxide nanoparticles were synthesized under an argon atmosphere via thermal decomposition of Fe²⁺-oleate complex. Exchange coupled Nd₂Fe₁₄B/ α -Fe nanocomposite magnets were prepared by reduction diffusion process. Exchange coupled Nd₂Fe₁₄B/ α -Fe nanocomposite magnets have been got the maximum energy product, (BH)_{max}.

EXPERIMENTALS

FeCl₂·4H₂O (99 + %) and sodium oleate (C₁₇H₃₃COONa, 98%) were obtained from Aldrich Chemical Co. and used without further purification. To prepare Fe²⁺-oleate₂ complex, 1.995 g of FeCl₂·4H₂O (10 mmol) was dissolved in deoxygenated water (200 mL, 18 M Ω , argon gas bubbling for 30 min). Resulting solution was added into 6.090 g of sodium oleate (20 mmol) under vigorous stirring for 2 hrs. The precipitate was separated by filtration and washed doubly with deionized water to be free of sodium and chlorine ions. After drying the iron-oleate complex was transferred into the pyrex tube. The complex was first flushed with argon gas, and then the tube was sealed at 0.3 Torr. The sample was slowly heated from room temperature to 300°C at 1°C/min. After reaching the desired temperature, it was held at 300°C for 2 hrs and cooled to room temperature. The complex color was changed from brown to black, indicating that Fe₃O₄ nanoparticles were being formed (yield = 100%). These metal nanoparticles can be easily redispersed in octane or hexane. When a permanent magnet was brought close to the flask, no movement of the particle solution was noticeable. This does not mean that the particles are not magnetic but only that the magnetic forces are much weaker than the viscous forces in solution. Because these fluids did not respond to a magnet, centrifugation was used to collect the particles following ethanol addition. The supernatant was decanted, and the particles were redispersed in hexane without additional surfactant because of oleate on the surface of nanoparticles [11].

Nd_2O_3 , and Fe_3O_4 rich (20 at%) were used as the starting materials for the synthesis of superfine neodymium oxide and iron oxide with metal oleate complex. The gels obtained were first treated at 250°C for 3 hrs in an oxygen atmosphere to remove all of the organic and other volatile components. The temperature was, then, increased to 500°C to convert the gels into oxides. A preliminary reduction treatment at 700°C under Ar-H gas, for 2 hrs, was applied to reduce Fe_3O_4 to the metallic states. Iron oxide with the stoichiometric ratios as in $\text{Nd}_2\text{Fe}_{14}\text{B}$ was used in the reactions. For compensating possible evaporating loss of neodymium metal during the reactions, 2 at% excess neodymium oxide was employed in the starting materials. In argon filled glove box the precursors were mixed with excess calcium hydride and transferred into a stainless steel crucible. To make the exchanged coupled magnetic nanocomposite, the reduction-diffusion reaction was carried out at 930°C for 2 to 4 h under purified argon [12].

ANALYSIS

To study the properties of the synthesized nanoparticles, we did various experiments. The crystal structure of the synthesized nanoparticles was identified by using X-ray powder diffraction (XRD) with a Philips X'Pert-MPD System with a Cu K_α radiation source ($\lambda = 0.154056\text{ nm}$). The size and shape of nanoparticles were obtained by transmission electron microscopy (TEM). TEM measurements were carried out on a HITACHI H-7500 low resolution TEM. Samples for TEM samples were prepared on 300 mesh copper grids coated with carbon. A drop of the nanoparticle solutions was carefully placed on the copper grid surface and dried. The size distributions of the particles were measured from enlarged photographs of the TEM images. Elemental analyses of them were conducted by using energy-dispersive X-ray microanalysis (EDX) on a JEOL JEM2010 TEM operated under an acceleration voltage of 200 kV.

Thermogravimetry using a microbalance with magnetic field gradient positioned below the sample was used for the measurement of a thermomagnetic analysis (TMA) curve showing the downward magnetic force versus temperature. In the TMA, sample was heated and cooled with rate of $7^\circ\text{C}/\text{min}$. The magnetization curves were characterized with Lake Shore 7300 vibrating sample magnetometer (VSM).

RESULTS AND DISCUSSION

The saturation magnetization, M_s , was determined as 186.5 emu/g for $\alpha\text{-Fe}$ nanoparticles as Figure 1, which is lower than that of bulk Fe, but

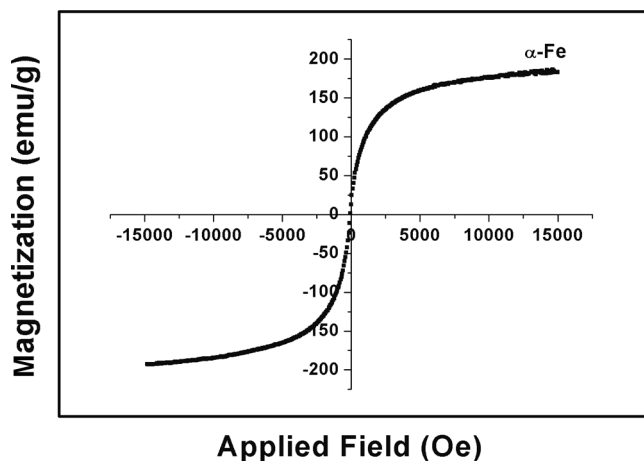


FIGURE 1 Vibrating sample magnetometer (VSM) curve of α -Fe nanoparticle.

indicates that Fe₃O₄ nanoparticle changed α -Fe nanoparticle. And a typical hysteresis loops for the Nd₂Fe₁₄B sample is shown in Figure 2. The coercivity is about 13 kOe. It should be noted to have permanent magnetic properties. The magnetic alloys of Nd₂Fe₁₄B have been known as best magnetic materials.

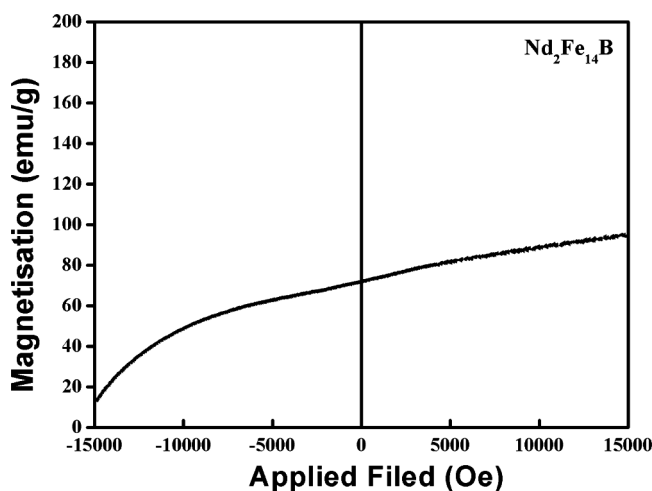


FIGURE 2 Vibrating sample magnetometer (VSM) curve of Nd₂Fe₁₄B nanoparticle.

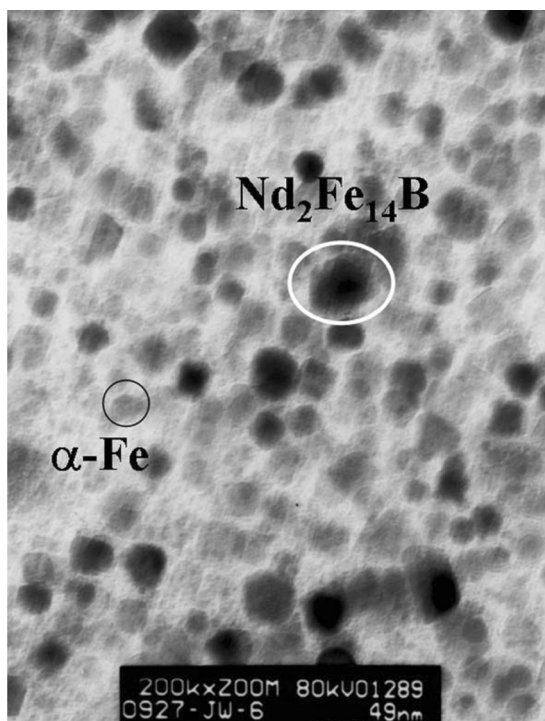


FIGURE 3 Transmission electron micrographs (TEM) image of $\text{Nd}_2\text{Fe}_{14}\text{B}/\alpha\text{-Fe}$ nanocomposite.

Figure 3 shows TEM images of $\text{Nd}_2\text{Fe}_{14}\text{B}/\alpha\text{-Fe}$ binary assemblies with fixed mass ratio of 5:1. $\text{Nd}_2\text{Fe}_{14}\text{B}/\alpha\text{-Fe}$ binary assembly shows locally clear mixed phase forming their own particle arrays. Figure 4 shows the EDX spectra of $\text{Nd}_2\text{Fe}_{14}\text{B}/\alpha\text{-Fe}$ nanocomposite excited by an electron beam (200 kV). Peaks for the elements of $\text{Nd}_2\text{Fe}_{14}\text{B}/\alpha\text{-Fe}$ were observed together with that for Cu. The Cu peaks are due to the 300 mesh copper grid. Usually, XRD can be used to characterize the crystallinity of nanoparticle.

In Figure 5, the XRD patterns clearly shows visible X-ray peaks corresponding to the crystallite formation of the compounds, $\text{Nd}_2\text{Fe}_{14}\text{B}$ (JCPDS card, no. 79-1994) together with the Fe (JCPDS card, no. 06-0696) peaks. They are consisted of a mixture of $\text{Nd}_2\text{Fe}_{14}\text{B}$ phase and $\alpha\text{-Fe}$ phase. Figure 6 shows TMA curve of the $\text{Nd}_2\text{Fe}_{14}\text{B}/\alpha\text{-Fe}$ nanocomposite magnet after annealing at 650°C . It can be seen that the material consists of the $\text{Nd}_2\text{Fe}_{14}\text{B}$ phase and $\alpha\text{-Fe}$ phase, as the same of the result of XRD spectrum as Figure 5. It can also be seen

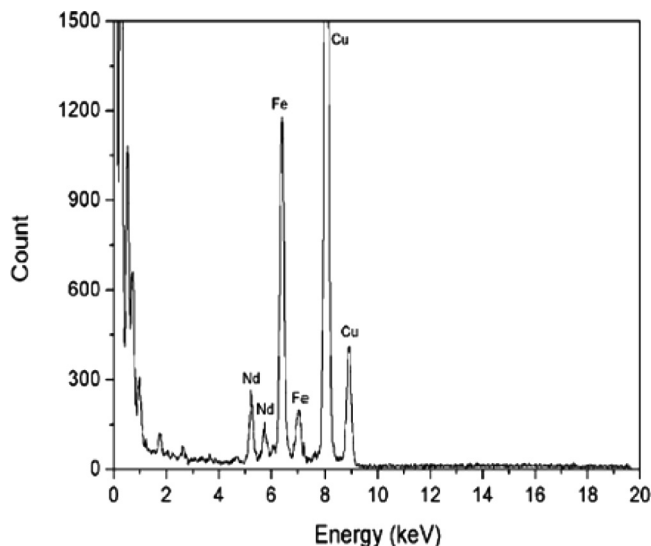


FIGURE 4 EDS patterns of $\text{Nd}_2\text{Fe}_{14}\text{B}/\alpha\text{-Fe}$ nanocomposite.

that the magnetization shows a maximum just below the Curie temperature (T_c) of $\text{Nd}_2\text{Fe}_{14}\text{B}$ phase of around 310°C . The microstructure of the $\text{Nd}_2\text{Fe}_{14}\text{B}/\alpha\text{-Fe}$ mixture consists of nanoscale $\text{Nd}_2\text{Fe}_{14}\text{B}$ and $\alpha\text{-Fe}$ grains. In such nanostructured material, no domain wall can

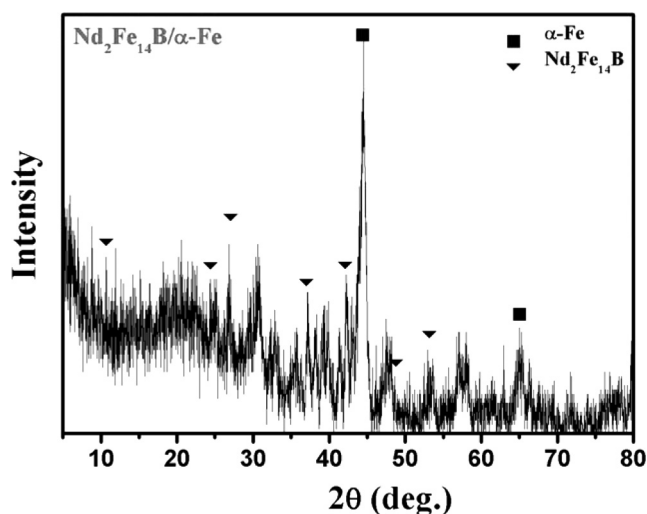


FIGURE 5 XRD patterns of $\text{Nd}_2\text{Fe}_{14}\text{B}/\alpha\text{-Fe}$ nanocomposite magnet.

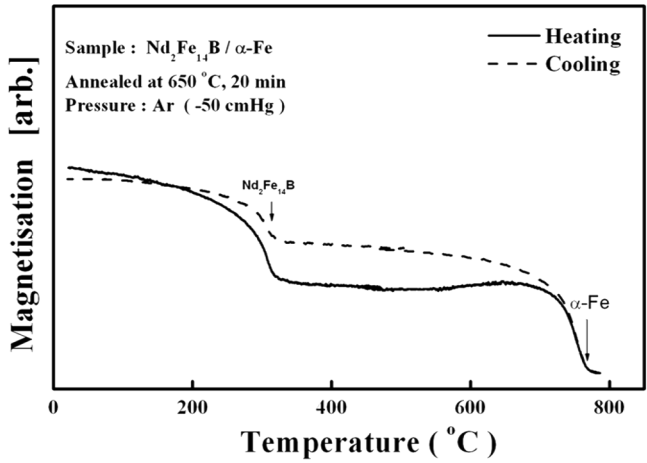


FIGURE 6 Thermomagnetic analysis (TMA) curve of the $\text{Nd}_2\text{Fe}_{14}\text{B}/\alpha\text{-Fe}$ nanocomposite magnet.

exist in the individual grains. When the sample is heated further towards the T_c of $\text{Nd}_2\text{Fe}_{14}\text{B}$, the magnetocrystalline anisotropy of the hard phase is reduced radically, thus magnetization rotation can take place much easily by the given applied field. As a result, the magnetization increases abruptly just below the T_c , and this is responsible

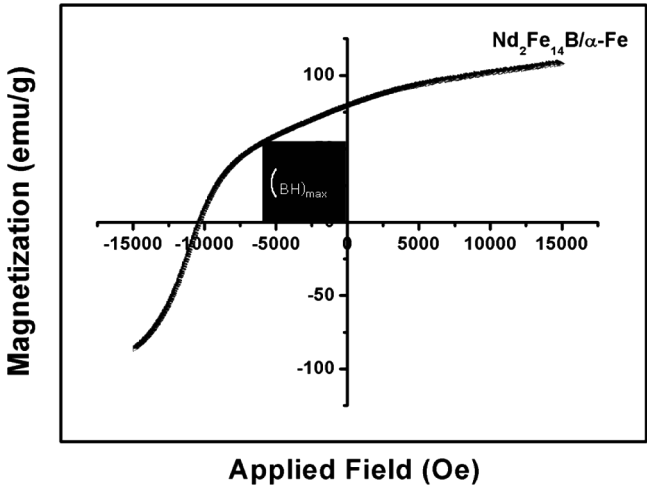


FIGURE 7 Vibrating sample magnetometer (VSM) curve of $\text{Nd}_2\text{Fe}_{14}\text{B}/\alpha\text{-Fe}$ nanocomposite.

for the magnetization maximum. The annealed sample shows a smooth demagnetization curve in Figure 7. It means that the milled material is typical of single-phase hard magnetic materials even though the sample consists of two distinctively different hard and soft magnetic phases. The smooth demagnetization curve is a consequence of a strong intergranular exchange coupling between the hard grains of Nd₂Fe₁₄B and soft grains of α -Fe grains in the sample.

CONCLUSIONS

The new synthetic method have been introduced to produce exchange coupled nanocomposite using thermal decomposition of Fe-oleate complex and reduction diffusion process, which were prepared by the reaction of FeCl₂ with sodium oleate in water solution and thermal treatment under argon gas. Herein, Nd₂Fe₁₄B/ α -Fe nanoparticles were prepared by reduction diffusion of metal oxide. Also, mono-dispersed α -Fe nanoparticles were synthesized under an argon atmosphere via thermal decomposition of Fe²⁺-oleate₂ complex. Exchange coupled Nd₂Fe₁₄B/ α -Fe nanocomposite magnets have been prepared by self-assembly using surfactant.

REFERENCES

- [1] Kneller, E. F. & Hawig, R. (1991). *IEEE Trans. Magn.*, 27, 3588.
- [2] Skomski, R. & Coey, J. M. D. (1993). *Phys. Rev.*, B 48, 15812.
- [3] Schrefl, T., Kronmuller, H., & Fidler, J. (1993). *J. Magn. Mag. Mater.*, 127, L273.
- [4] Coehoorn, R., De Mooij, D. B., & De Waard, C. (1989). *J. Magn. Mag. Mater.*, 80, 101.
- [5] Ping, D. H., Hono, K., & Hirose, S. (1998). *J. Appl. Phys.*, 83, 7769.
- [6] Kobayashi, T., Yamasaki, M., & Hamano, M. (2000). *Appl. Phys.*, 87, 6579.
- [7] Gong, W., Hadjipanayis, G. C., & Krause, R. F. (1994). *J. Appl. Phys.*, 75, 6649.
- [8] McCormick, P. G. (1998). *J. Appl. Phys.*, 83, 6256.
- [9] Zhang, J., Zhang, S. Y., Zhang, H. W., Shen, B. G., & Li, B. H. (2001). *J. Appl. Phys.*, 89, 2857.
- [10] Kwon, H. W. & Park, S. U. (2000). *J. Alloys and Compds.*, 302, 261.
- [11] Lee, D. K., Kim, Y. H., Zhang, X. L., & Kang, Y. S. (2006). *Current Appl. Phys.*, 6, 786.
- [12] Lin, J. H. & Liu, S. F. (1997). *J. Alloys Compds.*, 249, 237.